PHYSICAL REVIEW B **93**, 121412(R) (2016)

Dephasing of an electronic two-path interferometer

Itamar Gurman, Ron Sabo, Moty Heiblum,* Vladimir Umansky, and Diana Mahalu
Department of Condensed Matter Physics, Braun Center for Submicron Research, Weizmann Institute of Science, Rehovot 76100, Israel
(Received 4 February 2016; published 28 March 2016)

This Rapid Communication was motivated by the quest for observing interference of fractionally charged quasiparticles. Here, we study the behavior of an electronic Mach-Zehnder interferometer at the integer quantum Hall effect regime at filling factors greater than 1. Both the visibility and the velocity were measured and found to be highly correlated as a function of the filling factor. As the filling factor approached unity, the visibility quenched, not to recover for filling factors smaller than unity. Alternatively, the velocity saturated around a minimal value at the unity filling factor. We highlight the significant role interactions between the interfering edge and the bulk play as well as that of the defining potential at the edge. Shot-noise measurements suggest that phase averaging (due to phase randomization), rather than single-particle decoherence, is likely to be the cause of the dephasing in the fractional regime.

DOI: 10.1103/PhysRevB.93.121412

Interference of multiple electron trajectories is generally used to better understand coherent electron phenomena and their dephasing processes. Yet, the implementation of a high visibility electronic interferometer faces challenges, such as restricting the number of trajectories and achieving sufficiently long coherence and thermal lengths. Therefore, chiral edge channels in the quantum Hall effect (QHE) regime [1], being one-dimensional-like channels running along the edge of a two-dimensional electron gas (2DEG), are ideal as distinct trajectories in electron interferometers [2–4]. Based on these edge channels, the electronic Mach-Zehnder interferometer (MZI) is a true two-path interferometer with the enclosed magnetic flux between the two paths controlling the Aharonov-Bohm (AB) phase [5,6]. Indeed, its practical success allowed innovative studies of coherence and dephasing [7–9] as well as studies of the nature of electron-electron interactions in the integer QHE regime [10,11].

If realized in the fractional QHE regime, the MZI interference can serve as a probe of the statistics of fractionally charged quasiparticles [12–16]. However, despite a continuous effort to observe interference in the fractional regime, it was never achieved. In an attempt to understand the absence of such interference, we mapped the linear and nonlinear interference visibilities as the filling factor approaches $\nu = 1$.

Experiments were conducted with a high mobility 2DEG, embedded in a GaAs-AlGaAs heterostructure with areal densities $n = (1.8–2.5) \times 10^{11}$ cm^{-2} and mobility of $(2.5–3.9) \times 10^6$ cm^2 V^{-1} s^{-1} at electron temperatures of (10–15) mK. The electronic MZI [see Fig. 1(a)] is defined by two quantum point contacts (QPCs), each acting as an electronic beam splitter, a modulation gate charged by $V_{\rm mg}$, which controls the area A pierced by the magnetic field B, and two drains—one inside the MZI (D2) and the other outside (D1). QPC1 splits the incoming electron beam into two paths, which interfere at QPC2, to be collected in by the two drains. Aharonov-Bohm interference oscillations depend on the enclosed magnetic flux $\Phi_{AB} = AB$ [17]. In addition, another QPC resides between the source and the MZI (not seen in the figure) and is used to separate the incoming edge channels such that different channels can arrive with different applied potentials. Moreover, this QPC allows for separating the outermost edge channel from the conducting bulk when $R_{xx} \neq 0$. The nonlinear transmission of the MZI is measured by applying dc + ac ($f_0 \approx 1$ MHz) to the source and measuring the ac component at D1. In turn, the transmission of the MZI obeys $t_{MZI} = t_1 t_2 + r_1 r_2 + 2\eta\sqrt{t_1 t_2 r_1 r_2}\cos(\Phi_{AB} + \varphi)$, where $t_i(r_i)$ is the transmission (reflection) probability of QPCi, φ is an arbitrary (but constant) phase, and η is a coherence coefficient ($0 \leqslant \eta \leqslant 1$, depending on temperature, path lengths, and their differences, etc.). The visibility of the MZI is defined as $\frac{t_{\rm max} - t_{\rm min}}{t_{\rm max} + t_{\rm min}}$, where $t_{\rm max(min)}$ is the maximal (minimal) phase-dependent transmission of the MZI. Maximum visibility is obtained for $t_1 = 1 - t_2$ with the most convenient working point being $t_i = 0.5$, resulting in $t_{MZI} = \frac{1}{2} + \frac{\eta}{2}\cos(\Phi_{AB} + \varphi)$, with η as the visibility.

With the outermost edge channel biased and the inner ones at ground potential, interference oscillations were measured in the linear ($V_{\rm dc} = 0$) and nonlinear ($|V_{\rm dc}| > 0$) regimes. A typical linear transmission as a function of $V_{\rm mg}$ with a visibility of $\eta = 65\%$ and an average of 0.5 is seen in the inset of Fig. 1(b). Similar interference data were observed by varying the external magnetic field instead of the area (not shown here). With $|V_{\rm dc}| > 0$, the visibility exhibited the familiar lobelike behavior as a function of $V_{\rm dc}$ [Fig. 1(b)] with distinct maxima and minima (a phase jump of π in the oscillation appeared at each minima) [18]. The exact mechanism behind this effect is still debatable [19–21], but it is commonly accepted that electron-electron interactions are responsible for the "self-dephasing" of the interferometer. Moreover, it has been suggested that the first minima of the visibility V_0 depends on the ratio between the velocity (v) and the average arm length (L) $-eV_0 = \frac{hv}{2L}$ (up to a numerical constant), where e is the electron charge and h is Planck's constant. However, whether the velocity is the drift or group velocity of the electrons flowing at the edge or maybe the velocity of the neutral modes arising due to interedge interactions [22] is still debated.

We start with a MZI with its edges defined by "wet etching" (down to the donor layer; dubbed *etched defined*) as shown in Fig. 1(a). Interference was measured at different filling factors $\nu = hn/Be$, controlled by varying the magnetic field while keeping the areal electron density n constant. The visibility

*Corresponding author: moty.heiblum@weizmann.ac.il

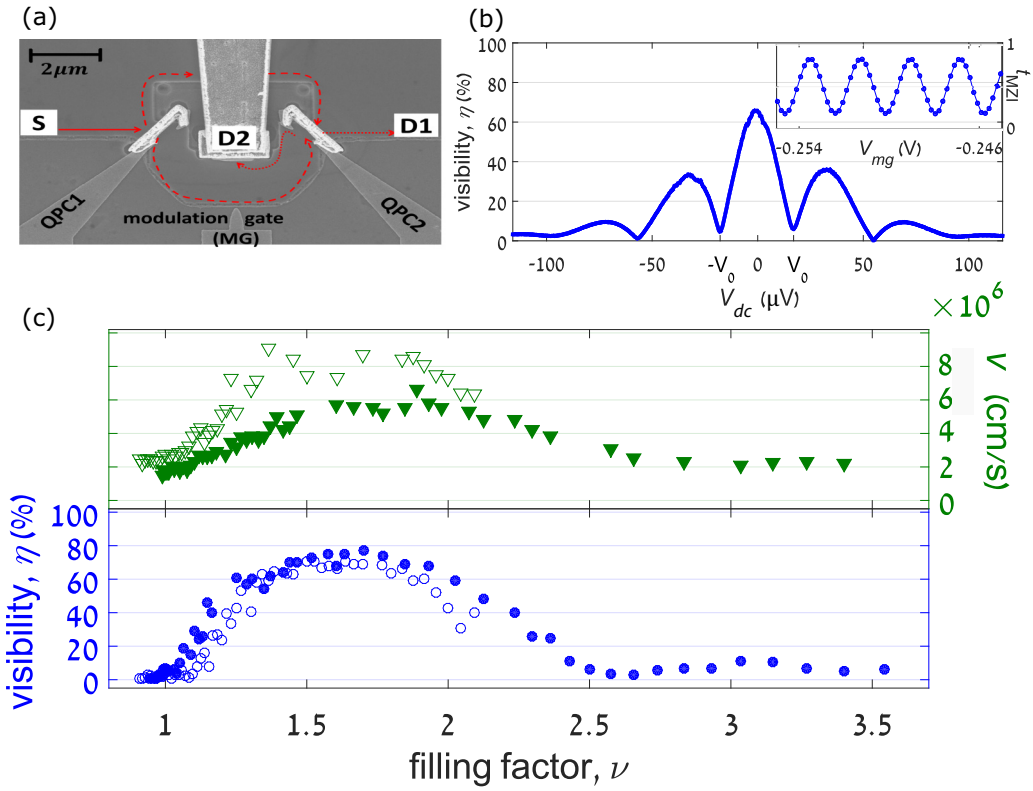

FIG. 1. Visibility in a mesa-defined Mach-Zehnder interferometer. (a) Scanning electron microscope (SEM) image of the MZI. The paths are defined using wet etching, QPC1 and QPC2 control the transmission of each electronic beam splitter and the modulation gate (mg) can modify the lower path such that it changes the enclosed area. The interfering channel (red arrows) can be biased either by a dc or an ac voltage, and the outcome of the MZI is either drained to the small Ohmic contact situated inside the interferometer (D2) or an external drain a few tens of micrometers away from it (D1). (b) Visibility of the oscillations as a function of $V_{\rm dc}$ (lobe structure). The voltage at which the visibility drops first to minimum is denoted by V_0 and proportional to the velocity. The inset: an example for measured sinusoidal oscillations at D1 while scanning $V_{\rm mg}$. (c) Visibility and extracted velocity (see the main text) dependence on exact filling factor $-\nu$. For each value of ν, the preselection QPC was set to fully transmit only the outermost channel and both interferometer's QPCs were tuned to half transmission. The visibility was extracted by scanning $V_{\rm mg}$ (blue circles), and the velocity was calculated using the nonlinear visibility (green triangles). Full and hollow shapes refer to different (yet similar) devices.

and the electron velocity of two such similar devices were plotted as a function of the filling factor in Fig. 1(c). A clear correlation between the visibility (blue circles) and the electron velocity (green triangles) is evident [23]. The visibility reaches a maximum around $\nu = 1.5$ and a minimum around $\nu = 2.5$; diminishing to zero as it approaches $\nu = 1$. The latter observation is surprising since the outer edge channel is still well defined with its conductance remaining within the $\sigma_{xy} = \frac{e^2}{h}$ plateau (bulk is still insulating). At the opposite end $\nu > 3.5$, we found a finite tunneling current between the edge channels (likely due to a smaller energy gap); therefore, the edge channels are not well defined. Noting, as the visibility goes down from 80% to 20% (factor of 4), the electron's velocity varies by a factor of 3. However, while the visibility keeps on quenching, towards full dephasing around $\nu = 1$, the velocity saturates at $v \approx 2 \times 10^6$ cm/s ($V_0 \approx 5\mu$V). The extracted velocities are an order of magnitude lower than the previously measured ones via edge magnetoplasmons excitation [24–26]. This discrepancy may be related to the interedge interactions (say, around $\nu = 2$), leading to slower neutral modes, which may dominate the periodicity of the "lobe structure" [20,22,27]. The fundamental observation of nonmonotonic dependence on the filling factor of both the visibility and the first lobe minima (V_0) was also reported in Ref. [23] where the focus was on the $0.9 \leqslant \nu < 2$ range.

Similar measurements were performed with the two paths confined by depleted regions under biased top gates [dubbed *gate defined*; inset in Fig. 2(a)]. In this MZI the confining potential is softer than the etched-defined one; yet, the dependence of the visibility on the bulk filling factor resembles (in general) the one in the etched-defined MZI. In addition, the velocity deduced from the lobe structure showed similar behavior and values as in the etch-defined version. A noted difference is the random phase jumps accompanying the periodic *AB* oscillations with an increasing rate as the filling factor approaches $\nu \approx 1$ [Fig. 2(a)—IV and V]. Once appearing, these phase jumps make the oscillations as a function of $V_{\rm mg}$ nonreproducible, unlike in the etch-defined device for which the interference pattern is stable even for visibilities lower than 1%. Furthermore, as the filling approached unity the phase jumps were more frequent, up to a point where even though the modulation gate's voltage was not altered the phase still spanned its full spectrum. This is as opposed to the $\nu > 1.5$ case where the visibility decreases in a smooth and a stable

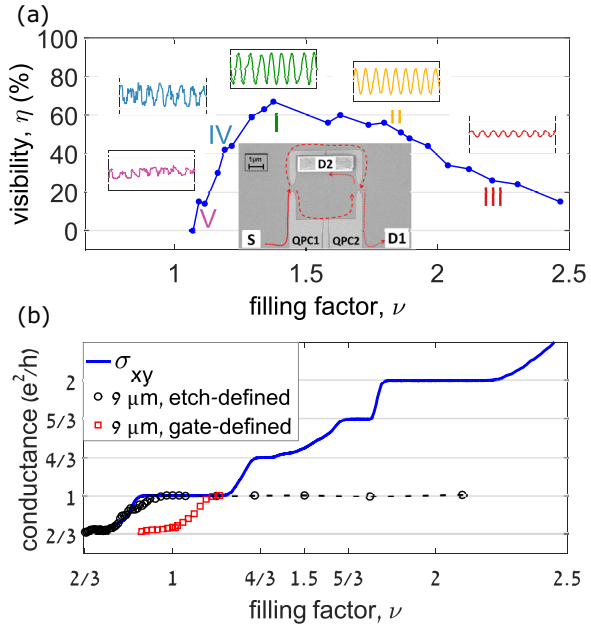

FIG. 2. Gate-defined Mach-Zehnder interferometer. (a) The visibility trend line as a function of filling factor shows a similar behavior to the one observed for the etch-defined device. The oscillation insets along points I–V demonstrate how the oscillations as a function of V_{mg} diminish in different ways, whether the filling factor is higher than 1.5, showing a smooth decline, or lower exhibiting random phase jumps with increasing rate (the transmission in the Y axis of all these insets is between 90% and 10%). The main inset: SEM image of the gate-defined MZI where the metal gates control both QPCs' transmission probabilities and define the two MZIs' paths (the two parts of each QPC as well as D2 are connected using an air bridge, which is not shown). (b) The conductance of the outer most edge as a function of the filling factor for both an etch-defined edge (black circles) and a gate-defined edge (red squares), whereas σ_{xy} is at the background (blue line). It is obvious to see that only the gate-defined case supports the formation of a $\frac{2}{3}\frac{e^2}{h}$ edge, despite σ_{xy} being at the $\frac{e^2}{h}$ plateau.

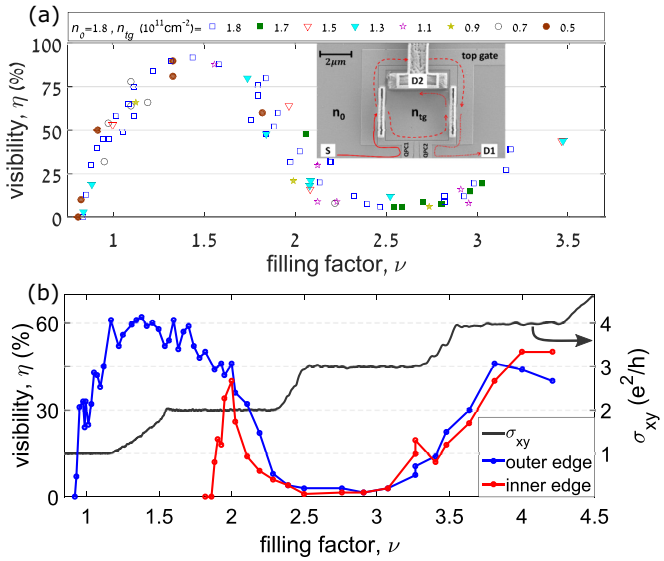

FIG. 3. (a) Visibility trend line in a gate-defined MZI with a top gate (the inset shows a SEM picture), which is used to change the local density n_{tg}. It shows the visibility does not solely depend on density nor on the magnetic field, but on the ratio between the two. Each marker represents a different value of n_{tg}. (b) Comparison of visibility trend line between outer edge (lowest spin-split Landau level, blue) and inner edge (second spin-split Landau level, red). Both trends are extremely similar down to $\nu = 2$ where the inner edge visibility decays in the same fashion outer edge visibility decays around $\nu = 1$. Notice that in the regime where more than two edges exist, we still compare only the two outermost ones. The dark gray line is the measured σ_{xy}.

manner [Fig. 2(a)—II and III]. As in the etched-defined MZI, no sign of interference was found at $\nu < 1$.

In order to understand the reason for the different behaviors of the two types of MZIs, the internal structure of the edge channels was studied in more detail. A "two-QPC" configuration, which allows probing the conductance of the outermost edge channel, was utilized [28–30]. For all integer states the conductance of the outermost edge was found to be $\frac{e^2}{h}$; namely, an integer channel of the lowest spin-split Landau level (LL). However, at bulk filling $\nu = 1$ the conductance of the outermost edge channel was found to be $\frac{2}{3}\frac{e^2}{h}$ in the gate-defined configuration [Fig. 2(b), red squares]. Note that the appearance of the phase noise coincides with the formation of the 2/3 channel at the edge with a likely counterpropagating neutral mode [29]. The correspondence of both phase jumps and a 2/3 edge mode can indicate the latter is the initiator of the phase instability. This can be explained by the partitioning of fractional charges, which in turn are likely to influence the phase accumulated in each arm [15]. Also, it was shown that the above nontrivial edge structure supports the formation of upstream neutral modes, which may cause energy relaxation and thus dephasing [29]. Contrary, in the etched-defined case, such a fractional state was not detected at the edge [Fig. 2(b), black circles] yet it could have been merged with the inner channel and thus not observed.

Does the characteristic behavior of the MZI depend only on the filling factor? To address this question, a gate-defined MZI with a top gate (biased V_{tg}) was fabricated, allowing control of the electron density ($0 < n_{tg} < n_0 = 1.8 \times 10^{11}$ cm^{-2}) in the MZI [Fig. 3(a)]. The visibility was found to depend solely on the local filling factor inside the MZI. Here too, an increasing phase noise appears once entering the $\nu < 1.5$ regime. In Ref. [23] a global *backgate* was utilized to change the electron density of the entire Hall bar, also proving that the key parameter that governs the visibility is the filling factor.

Whereas all the data presented thus far were of the outer most edge channel (the lowest spin-split Landau level), it is interesting (and challenging) to check its universality by interfering the next inner edge channel (second spin-split Landau level), which appears once $\nu \geqslant 2$. In Fig. 3(b) we show the visibility of the outermost edge channel (blue) and the next inner one (red). The two dependencies almost overlap. Here too, once crossing the $\nu = 2$ filling (thus entering fractional states of the second spin-split LL) the visibility of the interfering inner edge channel quenches with an escalating phase noise. Note that a high visibility interference of an inner edge is not typical and only seldom observed.

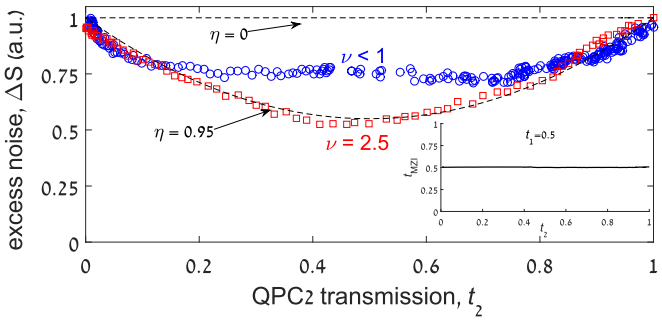

FIG. 4. Excess shot-noise measurements of a MZI which shows no oscillations. t_1 was set to be 0.5 such that $t_{MZI} = 0.5$, the source was biased with a constant dc voltage (50–80 μV), and t_2 was scanned from 1 to 0, either for $\nu < 1$ (blue circles) or for $\nu = 2.5$ (red squares). In both cases η is high (approximately 0.7 for $\nu < 1$ and 0.95 for $\nu = 2.5$), which shows that the visibility is null mainly due to phase averaging. The dashed lines are the excepted noises for $\eta = 0.95$ and $\eta = 0$. All noise data were normalized by the maximal measured noise, achieved at $t_2 = 0$, 1. The inset: an example (in this case for $\nu < 1$) how the total MZI transmission does not depend on t_2.

What is the reason for the disappearance of the interference oscillation at $\nu \leqslant 1$ and near $\nu = 2.5$? Does every electron lose coherence (hence, $\eta = 0$), or maybe, each electron acquires a random phase and thus phase averaging destroys the observed interference [namely, $\langle\cos(\Phi_{AB} + \varphi)\rangle = 0$]? Understanding of the relevant dephasing mechanism might be crucial for a possible recovering of the fractional interference. Alas, null visibility cannot distinguish between these two mechanisms. Yang *et al.* argued [6] that *shot-noise* measurements can be utilized to distinguish between these two dephasing mechanisms. Recalling the electronic excess noise density $\Delta S = 2eI\ t_{MZI}(1 - t_{MZI})\alpha(T)$ with I as the impinging current and $\alpha(T)$ as a reduction factor due to finite temperature [31,32], tuning $t_1 = 0.5$ and varying t_2, the device's transmission is $t_{MZI} = \frac{1}{2} + \eta\sqrt{t_2(1-t_2)}\cos(\Phi_{AB} + \varphi)$. The expected excess noise is then $\Delta S = 2eI\alpha(T)[\frac{1}{4} - \eta^2 t_2(1-t_2)\cos^2(\Phi_{AB} + \varphi)]$; hence, strongly dependent on η. If phase averaging is dominant, $\langle\cos^2(\Phi_{AB} + \varphi)\rangle = 0.5$, the excess noise will have a parabolic function of t_2. Alternatively, if single electron decoherence is dominant ($\eta = 0$), the excess noise will be independent of t_2. The considerable contrast between the two scenarios exemplifies the potency of noise measurement with a dephased MZI.

Performing noise measurements at $\nu < 1$ and with $t_1 = 0.5$, the normalized excess noise exhibits a clear t_2 dependence (Fig. 4, blue circles)—although not parabolic. Alternatively, around $\nu = 2.5$ (Fig. 4, red squares) the noise is parabolic with $\eta = 0.95$. Evidently, phase averaging plays a major role in the dephasing of the interferometer. It is worth mentioning that in all the cases when interference vanished (due to high temperature [6] with an asymmetric MZI with an Ohmic contact inserted in one path [33] and at various fractional quantum Hall states), we had found a parabolic noise dependence on t_2 with $\eta > 0.7$ - but never observed $\eta = 0$.

A variety of previous experimental works tried to understand dephasing by forcing it via an artificial environment, for example, by elevating the temperature [34], applying a finite dc bias [35,36], lengthening lengths of the trajectories [37], and inducing current fluctuations in nearby the chiral edges channels [10,38]. Here, we mapped the dependence of the visibility on intrinsic parameters of the system, such as the magnetic field, the electron density, the potential edge profile, and the actual interfering Landau level. Although the presented results do not single out the reason(s) for lack of interference in the fractional regime, a few important observations should be highlighted: (i) The visibility and the "chiral velocity" trend similarly as function of the filling factor, suggesting that lower velocity is accommodated with stronger dephasing. A longer dwell time in the MZI can account for the drop in the visibility. Moreover, as lower velocity is associated with a weaker confining electric field at the edge, phase averaging due to a "spatially wider edge channel" is also likely. (ii) The universal absence of any interference pattern at filling lower than one may suggest, e.g., that lack of screening of charge fluctuations at the bulk may have a dramatic effect on the interference [39,40]. (iii) A fractional state ($\upsilon = 2/3$) is formed near a soft edge as the bulk filling is close to one—simultaneously with an appearance of random phase jumps. Such fractional hole-conjugate states, mutually supporting neutral and fractionally charged excitations, may be the dephasing agents of the interferometer. (iv) Loss of interference, in particular in the fractional regime, likely results from phase averaging, whereas each quasiparticle's state maintains its own coherence. Not being a fundamental incoherent process of the fractional excitations, there is a ray of hope in observing interference by minimizing the averaging effects.

M.H. acknowledges partial support from the Minerva Foundation, the German Israeli Foundation (GIF), and the European Research Council under the European Community's Seventh Framework Program (FP7/2007-2013)/ERC Grant Agreement No. 339070. I.G. is grateful to the Azrieli Foundation for the award of an Azrieli Fellowship.

I. Gurman and R. Sabo equally contributed to this Rapid Communication.

[1] D. Yoshioka, *The Quantum Hall Effect* (Springer, Berlin, Heidelberg, 2002).

[2] F. E. Camino, W. Zhou, and V. J. Goldman, Quantum transport in electron Fabry-Perot interferometers, Phys. Rev. B **76**, 155305 (2007).

[3] M. Henny, S. Oberholzer, C. Strunk, T. Heinzel, K. Ensslin, M. Holland, and C. Schönenberger, The fermionic Hanbury Brown and Twiss experiment, Science **284**, 296, (1999).

[4] E. Bocquillon, V. Freulon, J.-M. Berroir, P. Degiovanni, B. Plaçais, A. Cavanna, Y. Jin, and G. Fève, Coherence and

indistinguishability of single electrons emitted by independent sources, Science **339**, 1054 (2013).

[5] M. Born and E. Wolf, *Principles of Optics*, 7th ed. (Cambridge University Press, Cambridge, UK, 1999), p. 348.

[6] J. Yang, Y. Chung, D. Sprinzak, M. Heiblum, D. Mahalu, and H. Shtrikman, An electronic Mach-Zehnder interferometer, Nature (London) **422**, 415 (2003).

[7] E. Weisz, H. K. Choi, I. Sivan, M. Heiblum, Y. Gefen, D. Mahalu, and V. Umansky, An electronic quantum eraser, Science **344**, 1363 (2014).

[8] I. Neder, M. Heiblum, D. Mahalu, and V. Umansky, Entanglement, Dephasing, and Phase Recovery via Cross-Correlation Measurements of Electrons, Phys. Rev. Lett. **98**, 036803 (2007).

[9] G. Haack, H. Förster, and M. Büttiker, Parity detection and entanglement with a Mach-Zehnder interferometer, Phys. Rev. B **82**, 155303 (2010).

[10] P. Roulleau, F. Portier, P. Roche, A. Cavanna, G. Faini, U. Gennser, and D. Mailly, Noise Dephasing in Edge States of the Integer Quantum Hall Regime, Phys. Rev. Lett. **101**, 186803 (2008).

[11] P.-A. Huynh, F. Portier, H. le Sueur, G. Faini, U. Gennser, D. Mailly, F. Pierre, W. Wegscheider, and P. Roche, Quantum Coherence Engineering in the Integer Quantum Hall Regime, Phys. Rev. Lett. **108**, 256802 (2012).

[12] V. V. Ponomarenko and D. V. Averin, Mach-Zehnder Interferometer in the Fractional Quantum Hall Regime, Phys. Rev. Lett. **99**, 066803 (2007).

[13] V. V. Ponomarenko and D. V. Averin, Braiding of anyonic quasiparticles in charge transfer statistics of a symmetric fractional, Phys. Rev. B **82**, 205411 (2010).

[14] P. Bonderson, K. Shtengel, and J. K. Slingerland, Interferometry of non-Abelian anyons, Ann. Phys. (NY) **323**, 2709 (2008).

[15] D. E. Feldman, Y. Gefen, A. Kitaev, K. T. Law, and A. Stern, Shot noise in an anyonic Mach-Zehnder interferometer, Phys. Rev. B **76**, 085333 (2007).

[16] K. T. Law, D. E. Feldman, and Y. Gefen, Electronic Mach-Zehnder interferometer as a tool to probe fractional statistics, Phys. Rev. B **74**, 045319 (2006).

[17] Y. Aharonov and D. Bohm, Significance of electromagnetic potentials in the quantum theory, Phys. Rev. **115**, 485 (1959).

[18] I. Neder, M. Heiblum, Y. Levinson, D. Mahalu, and V. Umansky, Unexpected Behavior in a Two-Path Electron Interferometer, Phys. Rev. Lett. **96**, 016804 (2006).

[19] M. J. Rufino, D. L. Kovrizhin, and J. T. Chalker, Solution of a model for the two-channel electronic Mach-Zehnder interferometer, Phys. Rev. B **87**, 045120 (2013).

[20] I. P. Levkivskyi and E. V. Sukhorukov, Dephasing in the electronic Mach-Zehnder interferometer at filling factor $\nu = 2$, Phys. Rev. B **78**, 045322 (2008).

[21] I. Neder and E. Ginossar, Behavior of Electronic Interferometers in the Nonlinear Regime, Phys. Rev. Lett. **100**, 196806 (2008).

[22] E. Bocquillon, V. Freulon, J.-M. Berroir, P. Degiovanni, B. Plaçais, A. Cavanna, Y. Jin, and G. Fève, Separation of neutral and charge modes in one-dimensional chiral edge channels, Nat. Commun. **4**, 1839 (2013).

[23] L. V. Litvin, A. Helzel, H.-P. Tranitz, W. Wegscheider, and C. Strunk, Edge-channel interference controlled by Landau level filling, Phys. Rev. B **78**, 075303 (2008).

[24] H. Kamata, T. Ota, K. Muraki, and T. Fujisawa, Voltage-controlled group velocity of edge magnetoplasmon in the quantum Hall regime, Phys. Rev. B **81**, 085329 (2010).

[25] M. Hashisaka, K. Washio, H. Kamata, K. Muraki, and T. Fujisawa, Distributed electrochemical capacitance evidenced in high-frequency admittance measurements on a quantum Hall device, Phys. Rev. B **85**, 155424 (2012).

[26] D. T. McClure, Y. Zhang, B. Rosenow, E. M. Levenson-Falk, C. M. Marcus, L. N. Pfeiffer, and K. W. West, Edge-State Velocity and Coherence in a Quantum Hall Fabry-Pérot Interferometer, Phys. Rev. Lett. **103**, 206806 (2009).

[27] H. Inoue, A. Grivnin, N. Ofek, I. Neder, M. Heiblum, V. Umansky, and D. Mahalu, Charge Fractionalization in the Integer Quantum Hall Effect, Phys. Rev. Lett. **112**, 166801 (2014).

[28] L. P. Kouwenhoven, B. J. van Wees, N. C. van der Vaart, C. J. P. M. Harmans, C. E. Timmering, and C. T. Foxon, Selective Population and Detection of Edge Channels in the Fractional Quantum Hall Regime, Phys. Rev. Lett. **64**, 685 (1990).

[29] V. Venkatachalam, S. Hart, L. Pfeiffer, K. West, and A. Yacoby, Local thermometry of neutral modes on the quantum Hall edge, Nat. Phys. **8**, 676 (2012).

[30] B. J. van Wees, E. M. M. Willems, C. J. P. M. Harmans, C. W. J. Beenakker, H. van Houten, J. G. Williamson, C. T. Foxon, and J. J. Harris, Anomalous Integer Quantum Hall Effect in the Ballistic Regime with Quantum Point Contacts, Phys. Rev. Lett. **62**, 1181, (1989).

[31] T. Martin and R. Landauer, Wave-packet approach to noise in multichannel mesoscopic systems, Phys. Rev. B **45**, 1742 (1992).

[32] R. de-Picciotto, M. Reznikov, M. Heiblum, V. Umansky, G. Bunin, and D. Mahalu, Direct observation of a fractional charge, Nature (London) **389**, 162 (1997).

[33] P. Roulleau, F. Portier, P. Roche, A. Cavanna, G. Faini, U. Gennser, and D. Mailly, Tuning Decoherence with a Voltage Probe, Phys. Rev. Lett. **102**, 236802 (2009).

[34] M. Hashisaka, A. Helzel, S. Nakamura, L. Litvin, Y. Yamauchi, K. Kobayashi, T. Ono, H.-P. Tranitz, W. Wegscheider, and C. Strunk, Temperature dependence of the visibility in an electronic Mach–Zehnder interferometer, Physica E **42**, 1091 (2010).

[35] L. V. Litvin, H.-P. Tranitz, W. Wegscheider, and C. Strunk, Decoherence and single electron charging in an electronic Mach-Zehnder interferometer, Phys. Rev. B **75**, 033315 (2007).

[36] E. Bieri, M. Weiss, O. Göktas, M. Hauser, C. Schönenberger, and S. Oberholzer, Finite-bias visibility dependence in an electronic Mach-Zehnder interferometer, Phys. Rev. B **79**, 245324 (2009).

[37] P. Roulleau, F. Portier, P. Roche, A. Cavanna, G. Faini, U. Gennser, and D. Mailly, Direct Measurement of the Coherence Length of Edge States in the Integer Quantum Hall Regime, Phys. Rev. Lett. **100**, 126802 (2008).

[38] A. Helzel, L. V. Litvin, I. P. Levkivskyi, E. V. Sukhorukov, W. Wegscheider, and C. Strunk, Counting statistics and dephasing transition in an electronic Mach-Zehnder interferometer, Phys. Rev. B **91**, 245419 (2015).

[39] H. le Sueur, C. Altimiras, U. Gennser, A. Cavanna, D. Mailly, and F. Pierre, Energy Relaxation in the Integer Quantum Hall Regime, Phys. Rev. Lett. **105**, 056803 (2010).

[40] C. Altimiras, H. le Sueur, U. Gennser, A. Cavanna, D. Mailly, and F. Pierre, Tuning Energy Relaxation along Quantum Hall Channels, Phys. Rev. Lett. **105**, 226804 (2010).